Available online at www.sciencedirect.com
ScienceDirect
Geochimica et Cosmochimica Acta 75 (2011) 483–499
Geochimica et Cosmochimica Acta
www.elsevier.com/locate/gca

Trace metal enrichments in Lake Tanganyika sediments: Controls on trace metal burial in lacustrine systems

Rebecca Poulson Brucker [a], James McManus [a,*], Silke Severmann [b,1], Jeremy Owens [b], Timothy W. Lyons [b]

[a] College of Oceanic and Atmospheric Sciences, Oregon State University, 104 Ocean Admin. Bldg., Corvallis, OR 97331-5503, USA
[b] Department of Earth Sciences, University of California, Riverside, CA 92521, USA

Received 10 September 2009; accepted in revised form 9 September 2010; available online 15 October 2010

Abstract

We investigate the distributions of several key diagenetic reactants (C, S, Fe) and redox-sensitive trace metals (Mo, Cd, Re, U) in sediments from Lake Tanganyika, East Africa. This study includes modern sediments from a chemocline transect, which spans oxygenated shallow waters to sulfidic conditions at depth, as well as ancient sediments from a longer core (~2 m) taken at ~900 m water depth. Modern sediments from depths spanning ~70–335 m are generally characterized by increasing enrichments of C, S, Mo, Cd, and U with increasing water depth but static Fe distributions. It appears that the sedimentary enrichments of these elements are, to varying degrees, influenced by a combination of organic carbon cycling and sulfur cycling. These modern lake characteristics contrast with a period of high total organic carbon (C_{org}), total sulfur (S_{Tot}), and trace metal concentrations observed in the 900 m core, a period which follows the most recent deglaciation (~18–11 ky). This interval is followed abruptly by an interval (~11–6 ky) that is characterized by lower C, S, U, and Mo. Consistent with other work we suspect that the low concentrations of S, Mo, and U may indicate a period of intense lake mixing, during which time the lake may have been less productive and less reducing as compared to the present. An alternative, but not mutually exclusive, hypothesis is that changes in the lake's chemical inventory, driven by significant hydrological changes, could be influencing the distribution of sedimentary trace elements through time.

1. INTRODUCTION

Lake Tanganyika is the largest of the East African Rift Valley lakes and is the second most voluminous body of freshwater in the world, with an estimated total volume of ~18,940 km^3 (Hutchinson, 1957). The lake occupies a ~650 km north–south trough that is ~50 km wide and ~1.4 km deep (Fig. 1; Edmond et al., 1993). Resting within the East African Rift Valley, Tanganyika harbors some amount of hydrothermal activity (e.g., Degens et al., 1971; Tiercelin et al., 1993). For example, Tiercelin et al. (1993) note the existence of shallow (<50 m) hydrothermal $NaHCO_3$ and NaCl springs in the northern sector of the lake. Despite these and other (Tiercelin et al., 1989; Barrat et al., 2000) hydrothermal features or signatures, within-lake hydrothermal activity is viewed as having relatively minor impact on the lake (e.g., Degens et al., 1971), and is not considered to play a dominant role in the lake's chemical properties (Cohen et al., 1997). Instead, the lake's chemical budget appears to be influenced by variations in river supply, most notably from the Rusizi (Cohen et al., 1997); however, weathering through other rivers can also be significant (e.g., Kimbadi et al., 1999). The Rusizi serves as drainage for Lake Kivu overflow, which is a volcanic lake and is a major alkaline source for many of the

* Corresponding author.
E-mail address: mcmanus@coas.oregonstate.edu (J. McManus).
[1] Present address: Rutgers University, Department of Earth and Planetary Sciences, Institute of Marine and Coastal Sciences, 71 Dudley Road, New Brunswick, NJ 08901, USA

0016-7037/$ - see front matter © 2010 Elsevier Ltd. All rights reserved.
doi:10.1016/j.gca.2010.09.041

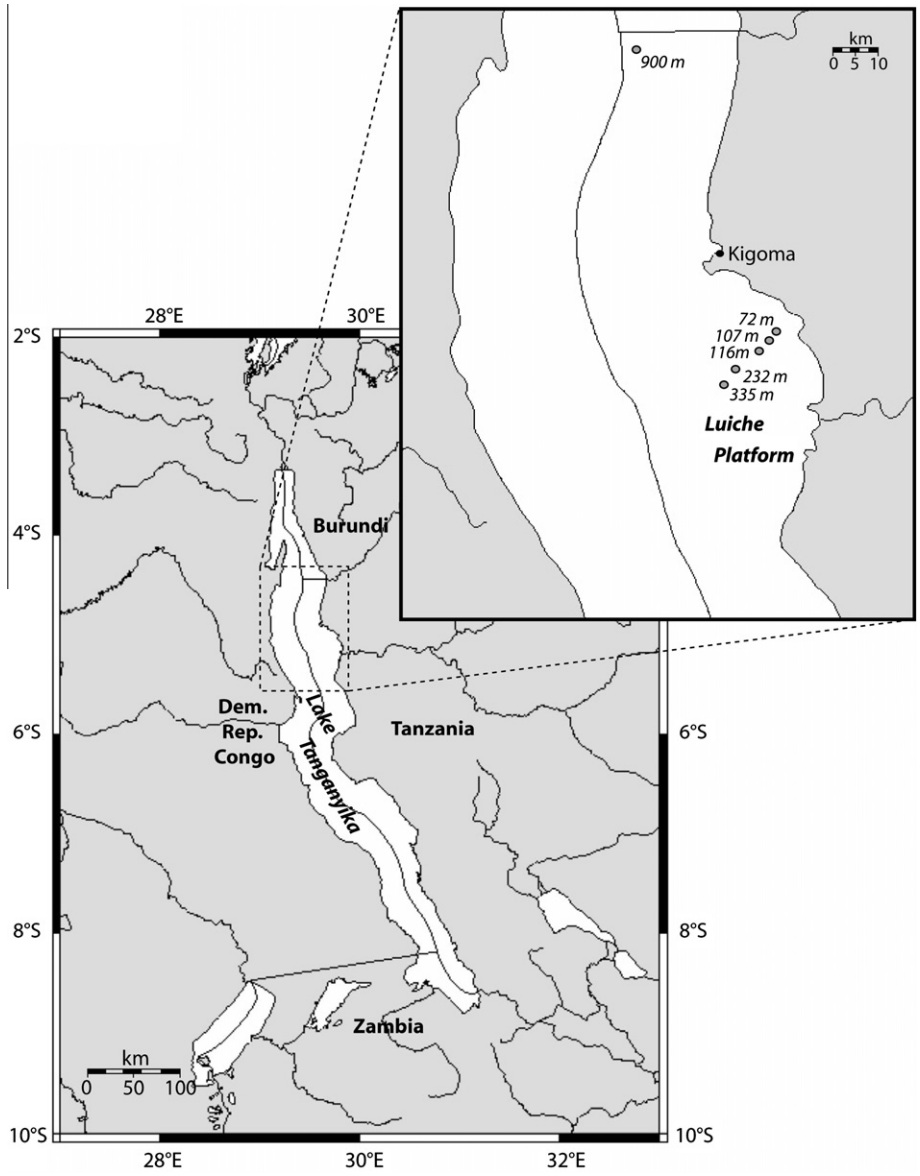

Fig. 1. Map of study area: Lake Tanganyika, Tanzania. Inset shows approximate location of the chemocline transect on the Luiche Platform, and the approximate location of the 900 m core. Corresponding core locations are: 72 m, 5.02249°S, 29.73979°E; 107 m, 5.03828°S, 29.72539°E; 120 m 5.05776°S, 29.72496°E; 232 m, 5.12086°S, 29.63161°E; 335 m, 5.16123°S, 29.59602°E; 900 m, 4.50308°S; 29.43546°E. Base map generated using www.aquarius.ifm-geomar.de.

Tanganyika's cations and anions (Craig, 1974; Stoffers and Hecky, 1978; Haberyan and Hecky, 1987; Cohen et al., 1997; Vandelannoote et al., 1999). Overflow from Kivu has not, however, been a constant feature, requiring relatively wet regional conditions (e.g., Stoffers and Hecky, 1978; Felton et al., 2007). Post-glacial overflow seems to have initiated around 10.6 ka with a possible cessation between 8 and 6 ka (Felton et al., 2007). The modern pH of Lake Tanganyika is ~8.5 (Edmond et al., 1993), and the upper water column is supersaturated with respect to calcium carbonate (Cohen et al., 1997). However, prior to about 2–4 ky there is effectively no, or very little, carbonate present within the sediments (Degens et al., 1971; Haberyan and Hecky, 1987; Felton et al., 2007), which implies a change in lake chemistry over the Holocene.

In addition to the riverine controls, the lake's internal chemistry is influenced by the combined effects of stratification and organic matter degradation, which produce strong chemical gradients (e.g., Edmond et al., 1993). During our field campaign in July 2006 the mixed layer penetrated to ~60 m with the oxycline effectively passing through our shallowest site (Fig. 2). As dissolved oxygen goes to 0 μM, sulfide concentrations increase, reaching a concentration of ~30 μM at ~300 m (Fig. 2, data from Edmond et al., 1993), and we refer to this chemical transition as the lake's chemocline. We do not have deep dissolved

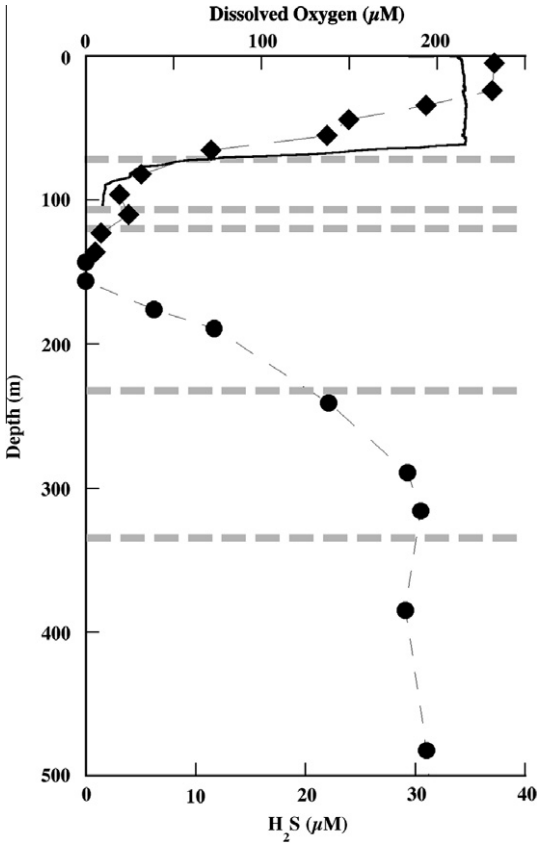

Fig. 2. Water column profiles from Northern Lake Tanganyika, Kigoma Basin. Diamonds are dissolved oxygen data from Edmond et al. (1993) and the dark line represents dissolved oxygen data collected using a CTD (data collected courtesy of Catherine O'Reilly). The CTD data were taken during 2006 around the time of our cruise near Kigoma (see Fig. 1). Filled circles are dissolved sulfide data from Edmond et al. (1993). Grey dashed lines indicate the approximate depth of cores collected for this study (Table 1).

oxygen or sulfide data from our field campaign, but historical data suggest that the transition between oxygen and sulfide occurs around 150 m water depth (Fig. 2) and historical measurements suggest that the depth of the chemocline may vary seasonally (Degens et al., 1971; Edmond et al., 1993). This latter point is supported by the observation that the thermocline is positioned at ~40–50 m water depth much of the year, but during the cool trade-wind season (April–September) mixing of surface waters deepens the thermocline to ~150 m (Huc et al., 1990; Edmond et al., 1993). The possibility of either seasonal or interannual variability in the chemocline depth necessitates some degree of caution, as chemical conditions in the overlying water column cannot be considered static. Despite sulfide concentrations that increase with depth, reported sulfate concentrations are relatively constant at ~40 μM throughout the water column, decreasing only slightly below ~1000 m water depth (Degens et al., 1971). Roughly constant sulfate comes as a surprise given the nearly equal quantity of sulfide in the deeper water column (Fig. 2; Edmond et al., 1993). It is noteworthy, however, that the scatter in the reported sulfate data (Degens et al., 1971) is high and the relatively constant nature of the water column concentration should be treated with some degree of caution as we suspect that at least some of this sulfate could be derived from oxidized sulfate prior to analysis.

In this study, we use Lake Tanganyika to address broadly relevant questions about the biogeochemical reactions that may lead to the sedimentary enrichment of Mo, U, Cd and Re in freshwater systems. In oxygenated aquatic systems, some trace elements are relatively soluble (e.g., Mo, U, and Re) whereas others may be less so (e.g., Fe). In the absence of dissolved oxygen, the more soluble elements can become relatively insoluble through changes in oxidation state, speciation, enhanced particle reactivity, or authigenic mineral formation (e.g., Froelich et al., 1979; Brown et al., 2000; Tribovillard et al., 2006). In addressing the factors governing the burial of our target trace metals, we examine the relationships among organic carbon, sulfur, and our target metals. To accomplish our goal of assessing geochemical variability across redox gradients we collected sediments across a depth gradient (~70–335 m water depth) that spanned the chemocline impingement off the Luiche Platform, a deltaic deposit off the eastern shoreline just south of Kigoma, Tanzania (Fig. 1 and Table 1). We also present data from a single deep site collected at ~900 m depth covering the period between ~5 and 18 ky.

2. METHODS

All sediment cores from the Luiche Platform were collected using a multi-corer—more specifically, a smaller version of that described by Barnett et al. (1984); the one used here collects four core liners. One core from each deployment was sectioned in the field under a nitrogen atmosphere and from this core we obtained sediment pore fluids, separated via centrifugation, as well as sediment solid phases. An additional core was sampled in the field for ^{210}Pb and ^{137}Cs analyses (see Electronic supplement). The core from the 900 m site was collected using a gravity corer. This core was cut into ~0.5 m sections and stored at the Oregon State Core Repository for later sampling and analysis.

Pore fluid trace metal analysis was done by quadrupole ICP-MS (Agilent 7500ce with collision cell) on diluted samples, using a standard calibration curve and internal standards for instrument drift correction. Riverine suspended particulate matter was collected along the Kalande Stream, which flows through the densely forested Gombe National Park and enters the lake at the northeastern shore. Samples were collected from a small boat from the river mouth to 200 m upstream. One liter samples were passed though a pre-combusted glass fiber filter and dried at 500 °C for 2 h before storage. After drying, the particles were carefully scraped off the filter with a clean scalpel to minimize filter-blank contributions. A small but un-quantified amount of glass fiber was also transferred for each sample, and to monitor this filter blank contribution we treated an unused filter the same way as the samples. The samples and glass fiber fragments were digested using a combination of HF–HNO_3–HCl mineral acids and analyzed on the UCR ICP-MS using the same analytical protocol as above. Filter blank contributions for Al and Cd were high, making a

Table 1
Sediment data for all Lake Tanganyika study sites.

Depth (cm)	C_{org}[a] (wt.%)	$CaCO_3$[b] (wt.%)	S_{inorg}[c,d] (wt.%)	±	C/N	Al (wt.%)	±	Ca (wt.%)	±	Fe (wt.%)	±	Ti (wt.%)	±	Mo (ppm)	±	U (ppm)	±	Cd (ppb)	±	Re (ppb)	±
Luiche Platform 72 m																					
0.25	3.4	40.4	0.01																		
0.75	2.9	47.7	0.04	0.05																	
1.5	2.6	45.8	0.04	0.05		5.32	0.28			4.6	0.2	0.38	0.00	0.57		1.80		70		1.9	
2.5	2.3	41.4	0.05	0.04																	
4.0	2.2	36.8	0.04	0.05		5.77	0.54			5.0	0.3	0.46	0.02	0.50	0.04	1.79	0.01	69	8	3.5	1.6
5.1	2.1	55.1	0.08	0.04																	
6.3	2.4	62.7	0.09	0.04		3.69				3.1		0.25		0.55		1.71		67		2.0	
7.4	2.2	67.9	0.07	0.02																	
8.6	2.2	65.6	0.08	0.02		4.54	0.51			3.5	0.1	0.27	0.01	0.61	0.05	1.72	0.05	52	6	2.1	0.1
9.7	1.9	65.8	0.07	0.04																	
10.9	1.5	73.1	0.05	0.07		2.95	0.22			2.4	0.2	0.19	0.00	0.43		1.73		34		1.6	
12.0	1.6	70.6	0.18	0.06																	
13.2	1.8	58.4	0.13	0.06		3.53	0.09			2.7	0.0	0.24	0.00	0.93		1.71		38		1.8	
14.3	1.9	58.9	0.13	0.03																	
17.5	3.4	29.1	0.15	0.06		4.99				4.0		0.35		0.74		1.87		54		2.3	
18.6	2.6	43.3	0.09	0.05																	
21.8	3.2	24.8	0.18			6.02				5.2		0.45		1.71		1.81		67		2.1	
22.9	2.7	37.1	0.16																		
26.1	3.7	14.8	0.16	0.02		7.70	0.21			6.3	0.1	0.54	0.01	0.67		1.82		77		2.2	
27.2*	3.7	13.0	0.17			9.04	0.61			7.0	0.1	0.60	0.02	2.06		1.67		75		2.6	
28.4	3.1	13.4	0.12																		
29.5	3.0	18.8	0.20																		
30.7	2.9	21.1	0.19	0.03																	
31.8	2.6	28.2	0.16	0.05																	
Luiche Platform 107 m																					
1.1	4.2	13.1	0.49	0.00		9.04				6.9		0.59		2.61		2.86		114		2.6	
2.3	4.1	11.7	0.56	0.03																	
3.4	4.0	13.9	0.58	0.11		9.18				7.1		0.60		0.98		2.71		177		2.9	
4.6	3.7	13.3	0.53	0.00		8.38				7.2		0.59		0.91		2.58		97		2.3	
7.7	3.4	55.7	0.40			4.30				3.4		0.27		1.01		2.48		54		2.7	
8.9	3.4	60.2	0.66			3.44				2.8		0.24		0.93	0.05	2.29	0.04	48	17	1.4	0.3
12.0	3.0	67.6	0.30			3.12				2.4		0.19		0.90		2.10		85		2.2	
13.2	3.7	58.1	0.59			3.81				3.0		0.24		1.01		2.30		31		1.9	
16.3	2.7	52.8	0.41	0.06		4.38				3.5		0.30		0.83		2.10	0.05	59	15	2.6	1.9
17.5	3.1	30.9	0.49	0.05		7.39				5.6		0.47		1.11		2.35		76		2.7	
20.6	3.1	41.0	0.50	0.06		5.68				4.3		0.37		0.92		2.23		93		2.7	
21.8	3.6	29.9	0.59			7.31				5.5		0.47		1.07		2.22		77		2.2	
Luiche Platform 120 m																					
0.6*	3.5	10.2	0.54	0.15		9.27				6.4		0.59		1.85		2.64		107		2.6	
1.2*	3.5	10.3	0.57			9.19				6.4		0.55		1.34		2.46		129		2.2	
2.3	3.4	9.2	0.62	0.11		9.09				6.6		0.54									
3.5*	3.0	10.0	0.77	0.12		9.04				6.9		0.55		1.83		2.69		96		2.9	
4.6	2.7	5.8	0.80	0.12																	
5.8	2.5	17.3	0.72			7.51				5.6		0.48		0.95		2.54		111		1.9	
6.9	3.4	25.7	0.52	0.12		7.73				6.0		0.47									
8.1	3.3	46.8	0.43			5.51				4.0		0.33		0.95		2.53		75		1.7	
9.2	3.2	57.9	0.36	0.03																	
10.4	4.0	54.8	0.37	0.05		4.40				3.2		0.25		1.13		2.34		52		1.9	
11.5	3.3	59.3	0.35	0.02																	
12.6	2.3	64.2	0.28	0.04		3.63				2.7		0.21		0.77		2.13	0.18	29	6	1.9	1.0
15.8	2.7	52.5	0.39	0.05																	
16.9	3.1	37.3	0.55			6.29				4.8		0.41		0.90		2.37		69		2.0	
20.1	2.1	43.5	0.41	0.02																	
21.2	2.6	28.7	0.59			7.49				5.6		0.49		1.03		2.42		75		1.9	
24.4	2.0	41.3	0.48	0.04																	
25.5	3.9	22.1	0.57			7.80				5.9		0.48									
26.7	4.8	5.3	0.69	0.09																	
27.8	4.4	5.7	0.74			8.30				7.3		0.65		1.16		2.27		101		1.6	

Table 1 (*continued*)

Depth (cm)	C_{org} [a] (wt.%)	$CaCO_3$ [b] (wt.%)	S_{inorg} [c,d] (wt.%)	±	C/N	Al (wt.%)	±	Ca (wt.%)	±	Fe (wt.%)	±	Ti (wt.%)	±	Mo (ppm)	±	U (ppm)	±	Cd (ppb)	±	Re (ppb)	±
29.0	4.8	4.6	0.69	0.07																	
30.1	4.7	4.7	0.64	0.05		7.49				6.9		0.63		1.37		2.30		100		1.9	
31.3	4.6	7.6	0.78	0.08																	
32.4	5.0	8.3	0.75	0.12		8.08				6.0		0.54									
Luiche Platform 232 m																					
0.6	6.3	0.0	0.62																		
1.2	5.6	4.6	1.07			9.91				6.5		0.55									
2.3	6.5	4.5	1.17	0.04		6.37				6.1		0.51		1.53		2.92		145		1.3	
3.5*	5.4	4.6	1.05																		
4.6	5.5	3.8	1.31	0.06		8.25				7.0		0.58		1.93		3.47		149		1.4	
5.8	4.6	7.8	1.22	0.15																	
6.9	4.0	23.1	1.16	0.04		8.61				5.8		0.46		1.74		3.33		123		1.4	
8.1	3.0	42.4	0.71	0.17																	
8.6	3.3	52.6	0.74																		
9.2	3.0	51.2	0.49	0.01		4.82				3.2		0.25						0		0.0	
10.4	2.4	62.9	0.53																		
11.5	3.9	48.7	0.64	0.05		4.50				2.9		0.22		1.57		2.68		62		2.4	
12.6*	2.7	62.7	0.47	0.07		3.51				2.3		0.19		2.03		1.92		47		2.2	
13.8	2.0	53.6	0.48	0.08																	
14.9	3.4	22.3	1.06	0.05		7.62				5.2		0.41		1.51	0.03	2.75	0.17	82	15	1.4	0.1
16.1	3.7	22.9	0.96	0.18																	
17.2	4.2	23.7	1.08	0.01		7.93				5.4		0.45		1.66		2.60		97		1.8	
18.4*	4.4	30.5	0.80	0.07		6.48				4.9		0.42		2.01		2.01		62		2.0	
19.5	4.1	17.9	1.26	0.20																	
20.7	5.6	6.1	1.12	0.19		8.52				6.5		0.57		1.66		2.29		110		1.5	
21.8	5.6	3.6	1.25	0.02																	
23.0	5.8	4.7	1.16	0.08		6.43				5.8		0.50		2.00		2.29		113		2.0	
24.1	6.9	0.0	1.21	0.08																	
25.3	4.5	24.6	0.85	0.04		6.89				4.5		0.40		1.37		2.42		85		1.7	
Luiche Platform 332 m																					
1.1	6.4	2.3	1.52	0.04		9.83	0.96			7.0	0.2	0.59	0.01	3.41	1.17	4.66	0.43	185	32	2.8	0.7
2.3	5.9	12.0	1.22	0.03																	
3.4	4.3	42.8	0.79	0.02		5.81	0.25			4.0	0.1	0.32		1.95		3.33		103		2.5	
4.6	4.4	52.6	0.79	0.03																	
7.7	3.7	63.1	0.55			3.40	0.24			2.3	0.1	0.19	0.00	1.88	0.46	2.44	0.16	55	10	2.3	0.1
8.9	4.6	58.7	0.75																		
12.0	5.3	29.5	0.91	0.05		7.39				5.1		0.41		2.05		2.96		98		3.3	
13.2	5.9	23.7	1.09	0.08																	
16.3	7.5	3.8	1.19	0.06		8.12	2.26			6.5	0.3	0.57	0.04	2.39	0.43	2.51	0.26	113	6	2.8	0.0
17.5	7.7	5.6	1.16	0.11																	
20.6	7.2	22.4	0.74	0.11		8.00	0.14			5.1	0.1	0.45	0.01	2.52	0.49	3.02	0.39	111	4	3.3	0.1
21.8	8.7	10.4	1.13	0.04		8.12				5.4		0.48		2.72		3.41		129		4.0	
	5.95		0.99																		
Northern Lake 900 m																					
1.5	12.0	0.8	2.76		20	7.83		0.50	0.26	8.1	0.4	0.37	0.04	4.65		5.90		378		8.0	
6.5	7.6	0.8	0.97		20	9.12		0.41	0.12	8.6	0.5	0.43	0.05	1.98		5.15		315		6.5	
16.5	5.9	0.8	0.27		19	10.53		0.35	0.05	7.9	0.3	0.49	0.05	1.38		5.37		296		3.4	
19.5	4.6	0.7	0.60	0.16		10.12		0.27		6.9		0.39									
26.5	5.9	0.7	1.40		22	10.03		0.35	0.07	7.5	0.6	0.48	0.07	1.64		5.14		316		4.7	
35.5	1.3	1.0	0.17	0.02	19	12.37	0.15	0.38	0.04	5.6	0.0	0.65	0.07	1.13	0.02	3.82	0.29	175	5	0.8	0.0
36.5	4.2	0.8	0.20	0.02	21	11.12	0.05	0.34	0.02	6.7	0.2	0.47	0.06	1.51	0.12	3.64	0.17	267	31	4.1	0.3
46.5	4.2	0.7	0.07	0.03	20	10.54	0.73	0.32	0.03	7.2	0.2	0.46	0.04	1.22		2.92		259		1.8	
56.5	5.6	0.7	0.88	0.33	23	11.92		0.30	0.01	5.6	0.1	0.51	0.05	1.93		3.75		317		4.0	
66.5	5.5	0.7	0.34	0.06	21	10.60	0.62	0.29	0.00	7.1	0.7	0.45	0.04	1.75		3.26		280		3.0	
76.5	7.2	0.9	0.37	0.17	24	11.36		0.35	0.04	6.4	0.1	0.47	0.04	2.13	0.10	3.56	0.02	272	21	2.7	0.2
86.5	10.7	0.9	2.36	0.02	32	10.97	0.20	0.35	0.01	5.7	0.0	0.46	0.03	2.84		3.62		398		6.3	
96.5	13.4	0.8	3.94	0.27	33	10.04	0.03	0.35	0.01	6.6	0.0	0.42	0.02	5.01		5.09		322		4.3	
106.5	15.7	1.1	2.60		34	9.89		0.43	0.04	5.4	0.0	0.41	0.03	4.26		5.64		303		4.5	

(continued on next page)

Table 1 *(continued)*

Depth (cm)	C_{org}[a] (wt.%)	$CaCO_3$[b] (wt.%)	S_{inorg}[c,d] (wt.%)	±	C/N	Al (wt.%)	±	Ca (wt.%)	±	Fe (wt.%)	±	Ti (wt.%)	±	Mo (ppm)	±	U (ppm)	±	Cd (ppb)	±	Re (ppb)	±
116.5	11.8	0.9	1.54	0.47	28	10.54	0.54	0.39	0.01	5.2	0.1	0.43	0.03	3.27	0.17	6.20	0.10	309	28	4.7	0.0
126.5	10.7	0.9	5.18	0.13	27	9.73	0.89	0.38	0.03	7.5	0.2	0.39	0.00	6.44		2.49		299		6.5	
136.5	12.0	1.4	3.81		25	9.10		0.50	0.08	6.3	1.1	0.39	0.03	6.78		3.64		301		7.3	
146.5	9.9	1.2	4.93		28	9.79		0.47	0.01	8.5	0.1	0.44	0.03	7.60		5.00		363		11.4	
156.5	5.3	0.9	0.68	0.03	26	11.11		0.38	0.03	6.1	0.1	0.49	0.03	1.61		3.41		287		3.8	
166.5	3.7	0.9	2.28	0.27	23	11.87	0.06	0.32	0.03	7.1	0.1	0.50	0.06	1.50	0.11	4.07	0.39	281	15	7.5	0.2
176.5	3.0	0.9	2.29	0.13	23	11.23	0.24	0.34	0.03	7.6	0.1	0.49	0.04	1.92		3.85	1.12	307	9	7.3	1.4
186.5	3.0	0.8	0.15	0.04	23	11.64	0.48	0.29	0.04	6.8	0.1	0.51	0.05	0.99		2.96		226		1.8	
196.5	2.2	0.7	0.11	0.01	21	11.84		0.25	0.02	6.2	0.2	0.51	0.04	0.90		2.68		191		1.3	

[a] C_{org} concentrations were calculated correcting TC for contributions from TIC, except for the deep 900 m site, were TIC was insignificant and no correction was applied.

[b] $CaCO_3$ concentrations were calculated from TIC, except for the deep 900 m site, where we use the total Ca concentrations instead.

[c] Mean S_{inorg} concentrations were calculated by combining TRIS from chrome reduction and TS from elemental analysis.

[d] ± uncertainties represent multiple (2 or more) digests or analytical determinations. In the case of S_{inorg} these are averages of two different types of determinations as described in the text.

reliable blank correction impossible, but blank contributions were generally <1% for Fe, Ti, and <5% for Mo and U, allowing us to calculate metal/Ti ratios in riverine particulates for this region.

For the 900 m core we measured ^{14}C on bulk sediments; the analysis was performed at the National Ocean Sciences Accelerator Mass Spectrometry Facility (NOSAMS) at the Woods Hole Oceanographic Institute (see Appendix Table S1 for ^{14}C results). We applied a reservoir correction following that used for Lake Tanganyika by Tierney et al. (2008), which is based on previously published efforts (Felton et al., 2007; Tierney and Russell, 2007). This correction is essentially a linear reservoir-versus-age relationship that decreases with time, yielding a ~570 year correction for the present to a correction of zero at ~15,500 years (reservoir correction in years = 569 − 0.037 × age). We calculated the calendar age using the radiocarbon age to calendar age program available at http://www.radiocarbon.ldeo.columbia.edu/research/radiocarbon.htm as described in Fairbanks et al. (2005).

Sediment samples were freeze-dried and ground before further analysis, with the exception of total reduced inorganic sulfur (TRIS) measurements, which were made on frozen wet sediment (Fossing and Jørgensen, 1989). Solid-phase trace metal and major element analyses were performed on ~100 mg of dry ground bulk sediment. Sediments were digested using a combination of HCl, HNO_3, and HF mineral acids in a microwave (CEM, MARS 5000) or were processed using a standard hotplate digestion procedure with HNO_3 + HF followed by HCl treatment. The bulk of the hotplate digestions were done at UCR and are primarily incorporated into the 900 m core results (Al, Ti, Ca, and Fe). For the 900 m core the two laboratory results (UCR and OSU) for Ti, Ca, and Fe were averaged. For Al, the OSU results of the 900 m core were systematically low and were not used in our analysis. The shallower cores were all digested at OSU, with most of those samples being digested via microwave. For the major elements the two methods generally agree within the analytical uncertainties (Appendix Table S3), with some notable exceptions. One important note is that the single run of the USGS reference material SGR-1, which was run at UCR, yielded low results (Table S3). In terms of the trace elements, there appeared to be some loss of Re from the PACS-2 (a modern marine sediment) and SDO-1 (a Devonian black shale) standard reference materials (SRMs), and some Cd loss from PACS-2 and perhaps SX-12280 (this latter sample being a siliceous laboratory sediment standard from 11°1.063′N, 140°4.8′W water depth 4921 m) when samples are digested via our hot plate method. This metal volatilization may occur during the pre-digestion treatment that includes a sample combustion step at 800 °C, which is not done for the microwaved samples. We do note however that these SRMs are not necessarily reflective of our matrix (in particular SDO-1, which has much higher concentrations of our target metals) (Appendix Table S3). With that concern we rely on the OSU (primarily microwave) results for the trace metals. We note here that there are a total of six samples (indicated in Table 1) that were not repeated via the microwave technique; given the manner in which we treat the data set, inclusion of these samples does not alter the conclusions of this study.

Major element compositions (Ca, Fe, Mn, Al, and Ti) were measured on total sample digestions by inductively-coupled plasma optical emission spectrometry (ICP-OES; Teledyne Leeman Prodigy) (Table 1). For the same bulk sediment sample digestions, trace metal concentrations (Mo, Cd, Re, U) were determined without preconcentration by inductively-coupled plasma mass spectrometry (ICP-MS; Thermo PQ ExCell) (Table 1). Major element concentrations analyzed by ICP-OES for the standard reference materials typically agree reasonably well with published values with the exception of the occasional sample (e.g., SGR-1, Table S3). Trace metal concentrations determined by ICP-MS on the standard reference materials generally agree reasonably well with reported values (Appendix Table S3). Replicate digestions and replicate measurements on lake sediment samples (Table 1) also imply that reproducibility for the major elements is generally better than ~10% (1SD; Table 1), while trace metal concentrations determined by ICP-MS were more variable (Table 1).

Total carbon (C_{tot}) and total sulfur (S_{tot}) were measured by bulk combustion using an elemental analyzer either at UCR (Eltra CS-500) or at OSU (Carlo Erba Instruments NA 1500) (Table 1 and Appendix Table S2). For the Luiche Platform cores, samples were acidified online for total inorganic carbon (C_{inorg}) (20% HCl), and total organic carbon (C_{org}) was calculated by difference (Table 1 and Appendix Table S2). For the 900 m core, C_{inorg}, which may be calculated from Ca measurements on total digests, is negligible and we presume C_{tot} measurements to approximate C_{org} contents (see Appendix Table S2). Samples for both C and N were analyzed for the 900 m core at OSU. For the Luiche Platform transect, both C_{org} and N were analyzed on a companion core from the same multicore deployment to the cores used for metal analysis, and the average C_{org}:N ratio from that data set is presented here.

In addition to the S_{tot} analyses (via an elemental analyzer as above), TRIS was measured using chromium reduction (Fossing and Jørgensen, 1989). Comparison of the entire data set from all sites shows a close correlation between the two S measurements (r^2) of 0.96 with a slope of 0.96 ± 0.03 (1σ) and an intercept of $0.07 \pm 0.04\%$ (see Table 1 and Appendix Table S2), which indicates that organically bound sulfur is negligible in these sediments. We average these two sulfur determinations together for this communication (termed S_{inorg} herein) and assume that these two determinations both represent the inorganic sulfur pool. For the deep core we do not have a complete data set for either sulfur analyte. Therefore, we merge both the TRIS and S_{tot} data from that core and present the data set as S_{inorg} as well.

3. RESULTS AND DISCUSSION

3.1. Age models

Sedimentation rates along the Luiche Platform are effectively indistinguishable from one another based on the ^{210}Pb profiles and ^{137}Cs (see Appendix for full discussion). In short, the three shallowest cores each have sedimentation rates that are closely clustered around 0.09 cm year^{-1}. For the 232 m core the upper portion of the core seems to have been lost, and the remaining ^{210}Pb data suggest a sedimentation rate of ~0.1 cm year^{-1}. For the 332 m core the ^{210}Pb data again suggest a rate of ~0.09 cm year^{-1}. We highlight our caution with our interpretation of these latter two rates as the data simply are not of the same quality as those for the three shallowest sites. In addition, alignment of the $CaCO_3$ maximums confirms the agreement among the three shallowest sites (~0.09 cm year^{-1}) with the 232 m site yielding a rate of ~0.07 cm year^{-1} and the 332 m site yielding a rate of ~0.05 cm year^{-1} (Poulson, 2008). In sum, sedimentation rates for the Luiche Platform sites appear to fall in a range of $\sim 0.08 \pm 0.03$ cm year^{-1}, and for our purposes we treat the rates here as approximately uniform but again point out that that treatment should be taken as an approximation. More specifically, for this work we do not calculate mass accumulation rates as the uncertainties in sedimentation rates as well as the other essential parameters used for that calculation (e.g., sediment density and porosity) are significant relative to the magnitude in variation.

The sediments in the 900 m core are generally dark gray to black with what appears to be mm-scale laminations. A thin (<1 cm) pale brown layer occurs at ~19.5 cm from the core top, and a similar but thicker brown layer is observed at ~34.5 cm. There also appears to be some reddish staining near the base of the core. The depth-versus-age relationship at the ~900 m site shows a generally linear trend from 0 to 150 cm (Fig. 3). A core-top age of ~5 ky suggests that the gravity core over-penetrated the sediment surface during coring. Also, we observe two anomalously high ages for the pale brown layers at ~19.5 and ~34.5 cm (Fig. 3 and Appendix Table S1). We interpret these older ages to reflect turbidite layers and the 34.5 cm point was excluded from our age model. We included the point at 19.5 cm since it does not deviate substantially from our trend, and this layer appears to be thinner. Likewise, there is a distinct layer of considerably older sedimentary material at the base of our core. We interpret these data (the bottom five data points) as also being influenced by turbiditic redeposition. We cannot rule out the possibility that there is a hiatus between the older sediments of this deeper layer and the more recent overlying material; however, the relatively uniform age of this layer is more consistent with a turbidite origin. We calculated a separate depth-versus-age relationship the four data points that span from 143 to 149 cm and extrapolated this trend to constrain the age of our deepest data point (i.e., there are two age points above and two below this data point; see below). We also note that these turbiditic intervals do not have distinct Ti-to-Al ratios (Fig. 3 and Table 1), implying a provenance for these sediments that does not differ significantly from that of the background sediment.

The generally linear trend between age and depth implies relatively constant sedimentation rate during the period from ~18 to 5 ky, with a noted decrease in sedimentation defined by the deepest (non-turbidite) data point. We note that this interpretation ignores potential changes in lithology, density, or porosity, which we did not measure and that may introduce some additional noise to our age model. The generally linear increase with depth suggests, however, that changes in the sediment composition do not appear to affect the sedimentation rate, except for the turbidites.

3.2. Sediment distributions

3.2.1. Organic carbon and sulfur

The average C_{org} concentrations increase from slightly less than 3 wt.% at the 72 m site to nearly ~16 wt.% at the 900 m site (Fig. 4 and Table 1). Lacking any data to verify or to the contrary, we assume that changes in surface productivity across the Luiche Platform are relatively small. Under this assumption it is possible that organic carbon concentrations may reflect at least some influence of an increase in material preservation as the sediments and their overlying bottom waters become more reducing (Fig. 2; Edmond et al., 1993). However, as indicated above changes in sedimentation rate could also influence any apparent preservation pattern, and as such there is simply insufficient data to unequivocally interpret simple enrichment (concentration) patterns as preservation patterns.

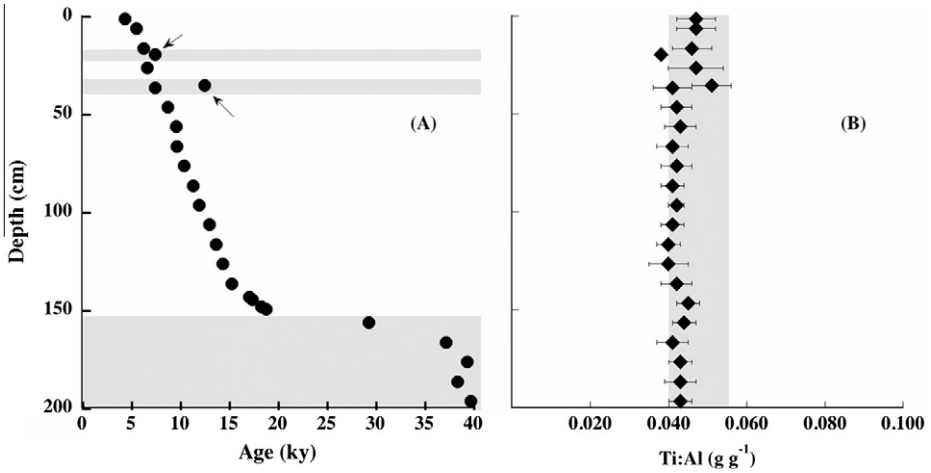

Fig. 3. (A) Depth as a function of sediment age for all the samples analyzed for ^{14}C analyses (data presented in Appendix Table S1). Samples that are shaded in grey appeared to be influenced by considerably older material than appropriate for the interval with the data at 19.5 and 35.5 cm being sediments that were distinctly lighter in color than the surrounding sediment. The point at 19.5 cm was included in the age model as this point appeared to be much less influenced by older material, although exclusion of this point does not significantly alter our age model. (B) Ti:Al as a function of sediment depth. The grey background covers a range in possible background values from 0.04 to 0.066. This range includes the average value from Taylor and McLennan, 1985, Table 8.2, as well as the values covered in their Table 5.1, which includes values up to 0.055.

There is a general assumption that the organic material in Tanganyika has largely been autochthonous in the past (Talbot et al., 2006; Felton et al., 2007). This contention is based on carbon isotope data, hydrogen indices, and carbon-to-nitrogen ratios (Talbot et al., 2006). Organic carbon and N analyses on companion cores from the Luiche Platform (data not shown) suggest little variation in C_{org}:N ratio along the platform with average molar ratios of $\sim 13 \pm 1$ (1SD, $n > 50$). These are at the lower end of the range of the southern lake ratios (~12–20) reported in Talbot et al. (2006) for the period between 10 and 22 ky at modern water depths of ~130 and 422 m. Our 900 m site ratios of 25 ± 5 (1SD, $n > 15$) (excluding those samples with anomalously high ages, Table 1) are somewhat higher than the shallow lake or published deep lake values. These ratios could imply a greater terrestrial component during this time period, a change in autochthonous stoichiometry, or a post-depositional alteration of the ratio. In any event, the difference between the Luiche Platform data and the older deep lake data illustrate the potential for a difference in the organic matter source. However, it is important to emphasize here prior contentions that despite these high ratios, the lake's organic material is thought to be largely autochthonous (Talbot et al., 2006).

Average S_{inorg} contents increase from ~0.1% at the 72 m site to as high as ~5% at the 900 m site (Fig. 4 and Table 1). Based on these data it is possible that sulfate reduction becomes increasingly important as a terminal electron accepting process with water depth and consequently that pyrite burial also increases with water depth. Unsulfidized reactive Fe concentrations of 1–5 wt.% in sediments from the Luiche Platform (measured as dithionite extractable Fe, Appendix Table S2) suggest that pyrite burial is not limited by Fe availability in the lake. Whole core average C_{org}:S_{inorg} ratios for the Luiche Platform sites decrease abruptly from the shallowest site (>20) to the subsequent deeper sites, where the average of each individual ratio is 6 ± 2 (1σ). This difference between the shallowest site and the others presumably reflects an increased importance of sulfate reduction and concomitant accumulation of iron sulfide phases (Fig. 5). In fact, whole core average C_{org} and S_{inorg} concentrations for all Luiche Platform sites generally trend along a similar slope, but the regression has a non-zero C_{org} intercept (Fig. 5). This non-zero intercept implies little or no net sulfate reduction at the shallowest site (Fig. 5). The combined slope for all the Platform sites is similar to the ratio for sulfate-rich oxic modern marine settings, which suggests that sulfate is not severely limiting in the lake (Fig. 5, after Berner and Raiswell, 1984). The low C_{org}:S_{inorg} ratios measured in sediments from all but the shallowest site suggest a similar relationship between sulfate reduction and organic carbon oxidation (Fig. 5).

In the 900 m core, C_{org}:S_{inorg} ratios are much more variable than those along the platform, with values as low as 1 and one value greater than 60 (Fig. 6). The observed C_{org}:S_{inorg} ratios are generally higher in the more recent Holocene sediment, and within the deep turbidite layer, with lower values in the older more carbon-rich deeper section. The higher C_{org}:S_{inorg} ratios in the upper section of the core appear to be driven by particularly low reduced sulfur contents in this interval (the C_{org} contents in this section are also relatively low compared to the deeper section). Notably, the low C_{org}:S_{inorg} ratios in the deeper section of the core corresponds to the highest sedimentary C_{org} and S_{inorg} contents, as well as significant trace metal enrichments (Table 1). These low C_{org}:S_{inorg} ratios suggest time periods when the deep basin may have been relatively rich in reduced sulfur.

3.2.2. Titanium and aluminum

Sediment Ti to Al ratios are generally uniform along the Luiche Platform with a value of 0.064 ± 0.008 (1σ). Despite this near-uniformity there is a trend of decreasing Ti:Al

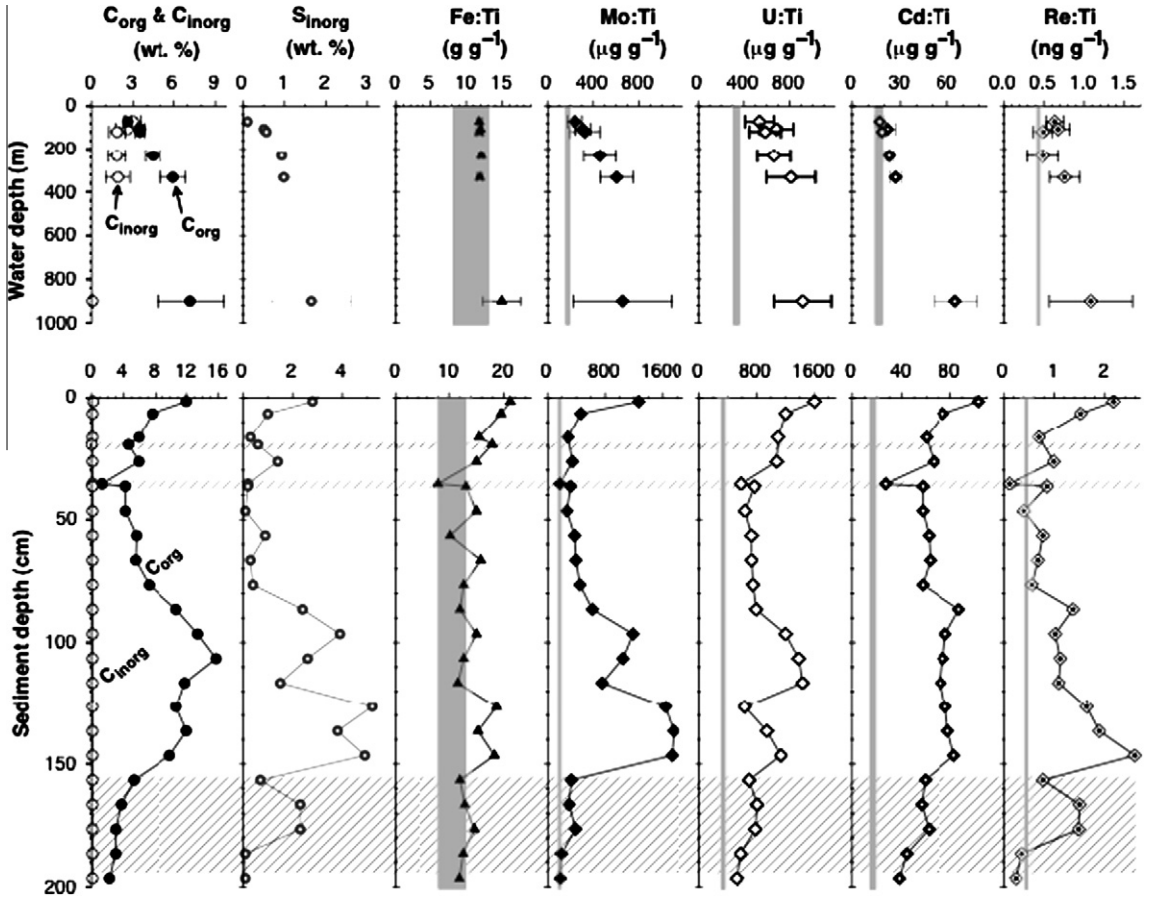

Fig. 4. (Top) Whole core average C_{org}, S_{inorg}, and metal to Ti ratios for all study sites. "Error" bars represent the standard deviation of the mean (2 SDOM) for whole core averages. Vertical grey and dashed lines indicate the spread in possible lithogenic metal:Ti ratio. For Fe the spread of values for the lithogenic background ranges from ~8 to 13, see text for discussion. For Mo this background envelope (grey bar) includes the lowest eight Mo:Ti ratios and the bulk crustal ratio ~185 μg g^{-1} from Rudnick and Gao (2004). For U this background envelope (two dashed black lines) ranges from ~270 to 405 and includes the seven lowest U:Ti ratios and the bulk crustal ratio ~301 μg g^{-1} from Rudnick and Gao (2004). For Cd this background envelope (grey bar) includes the lowest eight Cd:Ti ratios (12–15) and the bulk crustal ratio ~19 μg g^{-1} from Rudnick and Gao (2004); note that this envelope also includes more than the eight lowest data, which we use to define our lithogenic value. For Re, there is less data, but here we show the lithogenic value based on the bulk crustal ratio ~40 ng g^{-1} from Rudnick and Gao (2004). Average values for the deep core excludes those values identified as being influence by the older sedimentation (e.g., turbidite). (Bottom) Downcore profiles for C_{org}, S_{inorg}, and metal to Ti ratios for for the 900 m site. Horizontal grey areas in the 900 m profile indicate presumed turbidite layers (see text for details). Vertical grey lines are the lithogenic background envelope as noted above.

ratios with increasing bottom depth with the three shallowest sites (72–120 m) averaging 0.066 ± 0.006 and the deeper two sites (~230–335 m) averaging 0.060 ± 0.009. This separation could be caused by the deposition of more dense minerals in the shallower, near-shore regions of the Luiche Platform (e.g., Brumsack, 2006). Also, these sediments are slightly elevated in their Ti contents compared to bulk crustal material, which have typical Ti:Al ratios of ~0.04–0.05 (Rudnick and Gao, 2004). The 900 m core has relatively invariant Ti:Al ratios (0.043 ± 0.001) and those values are more typical of upper crustal ratios (Rudnick and Gao, 2004).

For our continued discussion here we will use Ti as a normalizing element rather than Al. Here the "normalizing element" provides us with an avenue for estimating the enrichment of trace metals over their crustal background (e.g., Brumsack, 2006). There are several reasons for using Ti rather than Al, although Al may generally be preferred (Brumsack, 2006). First, if there is some density sorting that preferentially deposits Ti in the shallow reaches, this process could also occur with other elements, for example Fe (see below). Second, and probably most importantly, the use of Ti does not alter the interpretations of trace metal enrichments, rather it provides a conservative view or a minimum estimate of the enrichments. Finally, we do present the Al data (Table 1) so that others may use those data to explore alternative interpretations of our data.

3.2.3. Iron distributions

Pore fluid iron distributions (Fig. 7) are surprisingly low. Concentrations in all the Luiche cores seem to increase slightly below ~10 cm depth, but the overall pattern of the pore fluid data implies that very little iron is escaping from the sediments via diffusion. This point follows from

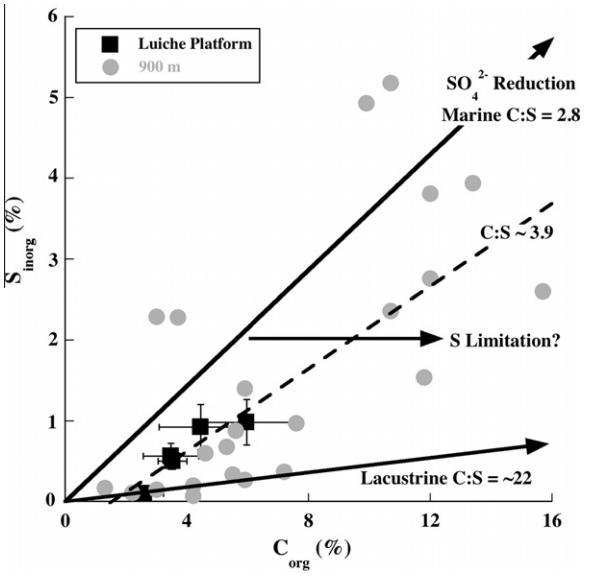

Fig. 5. Whole core average sediment S_{inorg} plotted as a function of C_{org} for all Luiche Platform study sites along with all the individual data points from the 900 m core. Errors are 1σ for whole core averages. Marine and lacustrine C:S values from Berner and Raiswell (1984). Dashed line represents fit to the Luiche Platform data resulting in a slope of 0.25 ± 0.07 ($R^2 = 0.83$) or a C:S ratio of 3.9.

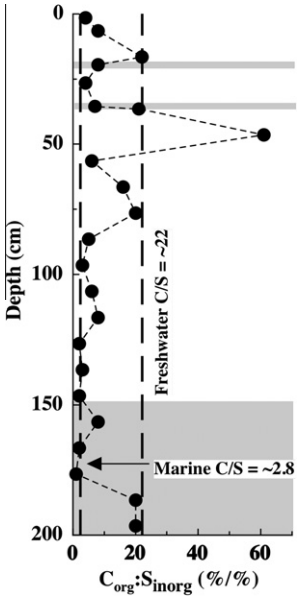

Fig. 6. Profile of C_{org} to S_{inorg} ratio (%/%) plotted as a function of depth for the 900 m core sediments. Marine and freshwater C:S values from Berner and Raiswell (1984). Grey areas indicate presumed turbidite layers (see text for details).

our point that unsulfidized reactive Fe concentrations are relatively high in these sediments, from 1 to 5 wt.% with an average of $2.6 \pm 0.9\%$ and no real trend with core depth (Appendix Table S2). Also in line with these observations, the solid-phase Fe:Ti ratios are relatively invariant at all Luiche Platform sites, averaging 11.9 ± 0.5 for all samples analyzed (Table 1). Whole core average Fe:Ti ratios are within the wide range reported values for Proterozoic fine-grained sedimentary rocks (Fe:Ti ~8–13; Taylor and McLennan, 1985) as well as the value for bulk crust (~12.1; Rudnick and Gao, 2004), but the Luiche Platform average is most consistent with an average value for upper continental crust (Fe:Ti ~11.7; Taylor and McLennan, 1985). The apparent invariance of measured Luiche Platform Fe:Ti ratios suggests that the sedimentary Fe pool at these sites is likely dominated by detrital Fe. However, and despite this contention, the suspended particle Fe:Ti ratio is low (6.2 ± 0.3, $n = 20$ plus two replicate samples, which we include in the average). We do not have a simple explanation for this difference beyond the possibility that these particular river particles are relatively Fe poor compared to sediment, or that these detrital sediments are not representative of the background sediment.

In contrast to the Fe:Ti ratio, sediment S_{inorg} contents increase with site depth (Fig. 4), consistent with the persistent exposure to sulfide and the progressive sulfidation of the Fe (Table 1; Raiswell et al., 1988). The observed increase in sedimentary reduced sulfur without an observable change in sediment Fe:Ti ratios suggests that there is little net iron dissolution from these sediments and therefore little or no redistribution of that iron via a shuttle mechanism (Wijsman et al., 2001; Anderson and Raiswell, 2004; Severmann et al., 2008). However, there is a possibility that the lack of Fe:Ti change with depth is because both of these elements maybe dominant in heavy minerals (Brumsack, 2006), and that physical processes are effectively conspiring to mask any change in the Fe:Ti ratio. Given the concordance between the background values along the Luiche platform with those of the deep Fe:Ti ratios (see below), this conspiracy seems remote. However, as is obvious from the slight depth gradient in Ti:Al, there is also a depth gradient in Fe:Al, with the most Fe-rich sediments in the shallower reaches of our transect—again, most like Ti. Although an iron enrichment pattern with depth of this manner is certainly possible, we might have expected the reverse pattern in that the higher dissolved sulfide concentrations present at 335 m would effectively titrate any pore fluid Fe, leaving the sediment package at this depth iron rich relative to the shallower sites. This expectation is akin to what is seen in the Black Sea, where sedimentary iron is remobilized along the (oxic) shelf and deposited in the deeper (sulfidic) basin (e.g., Severmann et al., 2008; Lyons and Severmann, 2006).

3.2.4. Trace metal distributions

Sedimentary trace metal concentrations include a contribution from terrigenous material, but for the purposes of our discussion we are interested primarily in the enriched or excess pools of metals, because they are the most sensitive indicators of changes in oxidation–reduction reactions and biogeochemical cycling. To calculate the excess metal component we estimate the background detrital fraction based on sediment Ti concentrations and an assumed background lithogenic metal-to-Ti ratio for each metal of interest (Figs. 4 and 8, and Appendix Table S2). We do not know of any trace metal data for bedrock within the study

area, so we use the lowest group of values measured in our cores to reflect the un-enriched detrital input. This approach was validated by comparison with bulk crustal values (e.g., Rudnick and Gao, 2004, their Table 9). In general the lowest values are weighted toward the shallowest core. The net effect is that we present our data as having an envelope that defines the possible range in background values (Fig. 4).

For Mo, the background envelope includes the lowest eight Mo:Ti ratios and the bulk crustal ratio of ~185 μg g^{-1} from Rudnick and Gao (2004). For calculating the excess Mo we use the average Mo:Ti ratio of the lowest eight points to reflect the detrital input: 157 μg g^{-1}. This ratio is greater than that measured in suspended sediment (47 ± 6 μg g^{-1}, $n = 22$, which includes two replicate samples). For U, the background U:Ti envelope ranges from ~270 to 405 μg g^{-1} and includes the seven lowest sediment U:Ti ratios and the bulk crustal ratio ~301 μg g^{-1} from Rudnick and Gao (2004). As is the case for Mo, the suspended particle U:Ti ratio is lower than these sediment ratios (92 ± 3 μg g^{-1}, $n = 22$). For Cd this background envelope (Fig. 4) includes the lowest eight Cd:Ti ratios (12–15) and the bulk crustal ratio ~19 μg g^{-1} from Rudnick and Gao (2004); note that this envelope also includes more than just the eight lowest values that we used to define our lithogenic value. For Re there is less literature data, and here we use the lithogenic value based on the bulk crustal ratio ~40 ng g^{-1} from Rudnick and Gao (2004).

We note here that our choice of background values maintains a degree of subjectivity as one could certainly rationalize a different choice. However, with the exception of Re, the lowest metal:Ti ratios typically occur in sediments from the shallowest, most oxic site on the Luiche Platform where (detrital) sedimentation is presumably highest and the enrichment mechanisms are least efficient (Fig. 4 and Appendix Table S2). In addition, our limited particle data are supportive of our choice as these ratios are nearly a factor of three lower than our choice of background. We therefore assume that the lowest measured metal:Ti ratios from our samples provide a reasonable, if not conservative, estimate of the sediment detrital metal fractions.

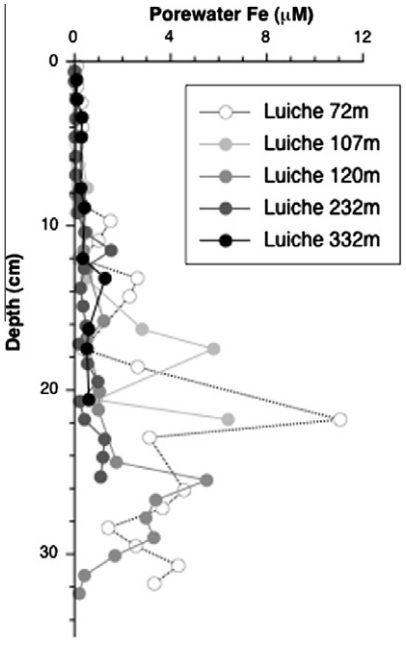

Fig. 7. Pore fluid iron profiles from the Luiche Platform cores.

Sediment metal concentrations enriched over the predicted lithogenic contributions are considered the "excess" fraction ($metal_{xs}$, Fig. 8 and Appendix Table S2). However, because the fraction of sedimentary carbonate varies throughout the Luiche Platform sites (from <5% to ~65%, Table 1), any metal incorporation into carbonate will influence sedimentary metal contents. In fact, sediment metal:Ti ratios appear to be influenced (to varying degrees) by carbonate contents, as there are coincident maxima in metal:Ti and carbonate concentrations suggesting the possibility that at least some contribution of carbonate-associated metals to the total sedimentary metal pool (Table 1). However, we choose not to make this correction because these metals tend to have low concentrations in carbonate minerals (e.g., Voegelin et al., 2009). Also, sediments from the 900 m site typically have carbonate contents less than about 1% (Table 1).

Some metals are considered biologically essential (Mo and Cd) or form associations with organic matter (U) (e.g., Anderson et al., 1998; Zheng et al., 2002; Tribovillard et al., 2004; Lane et al., 2005; Algeo and Lyons, 2006; Mendel and Bittner, 2006), therefore metal contributions associated with deposition of organic matter are likely to be important in these sediments. Molybdenum serves a variety of biochemical functions and is notably important for nitrogen fixation (e.g., Mendel and Bittner, 2006; Morel, 2008; Glass et al., 2009, 2010). Because of biological Mo requirements of phytoplankton, the natural pool of organic matter will inherently contain some assimilatory Mo (Tuit et al., 2004; Glass et al., 2010). In fact, natural nitrogen fixing populations may maintain Mo pools in excess of that considered biologically essential (Glass et al., 2009, 2010). For example, *Trichodesmium* cultures have Mo:C_{org} ratios of ~2 μmol mol^{-1}, which seem to reflect their biological requirement, but field samples can be a factor of 10 greater than this value (Tuit et al., 2004). Freshwater systems typically have low dissolved Mo concentrations, which could lead to limitation of available Mo (Goldman, 1960; Howarth and Cole, 1985; Glass et al., 2010), and indeed our own measurements on the overlying water of our cores exhibit a Mo concentration of 3.4 ± 1.3 nM ($n = 9$).

Although we do not distinguish among the different enriched pools, the biological Mo pool should be distinct from syngenetic or diagenetic metal enrichments. These latter pools represent the Mo that is incorporated into particles through abiotic processes (surface adsorption or authigenic mineral formation), which may occur in the water column or in the sediments. In the presence of sulfide, soluble Mo species (e.g., MoO_4^{2-}) are converted to less soluble thiomolybdates ($MoO_xS_{4-x}^{2-}$) that may be removed by organic matter or Fe-sulfide phases such as pyrite (Helz et al., 1996; Zheng et al., 2000). Based on experimental work, Helz et al. (1996) and Erickson and Helz (2000)

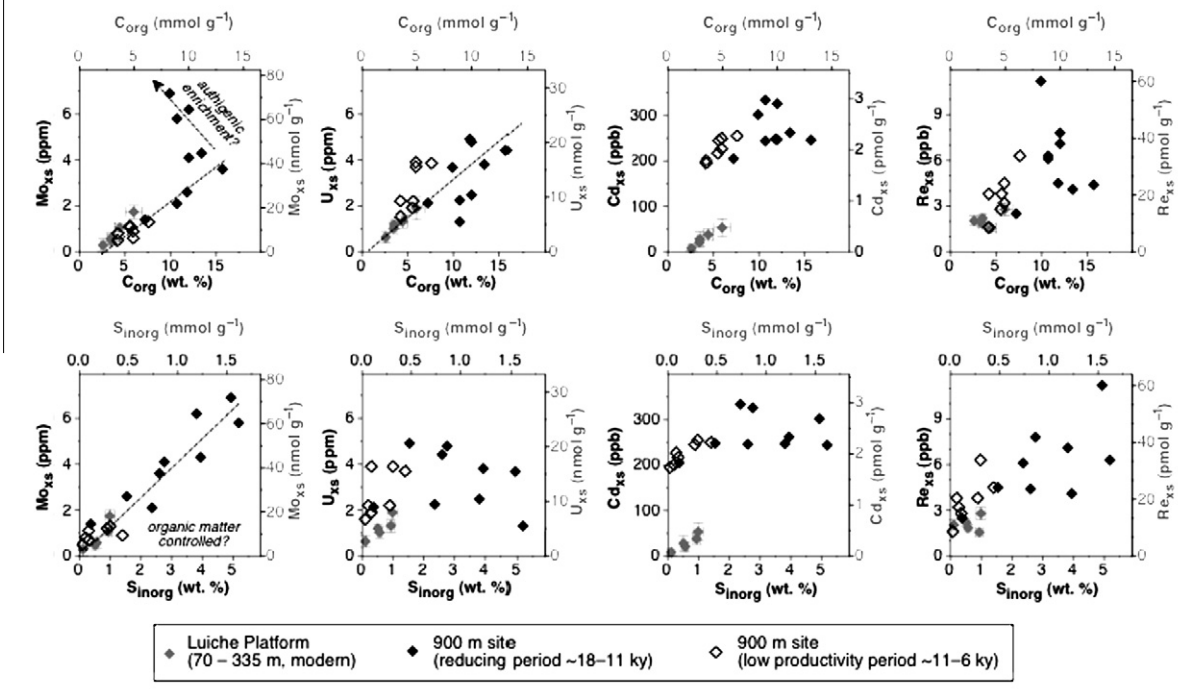

Fig. 8. Sediment trace metal enrichment data plotted as a function of organic carbon (top panels) and inorganic sulfur (bottom panels). Note that the grey axes are the same property with different units. Light grey data points represent Luiche Platform averages whereas darker points are from the 900 m core.

proposed a marine sulfide-controlled action point switch (APS) for Mo at 11 ± 3 μM $H_2S_{(aq)}$ (equivalent to ΣH_2S of ~100 μM at seawater pH), where the dominant dissolved Mo phase transitions abruptly from molybdate (MoO_4^{2-}) to tetrathiomolybdate (MoS_4^{2}). Work by Zheng et al. (2000) on natural marine samples suggests two thresholds for Mo-sulfide formation; coprecipitation of Fe–Mo–S phases at ~0.1 μM ΣH_2S, and Mo precipitation independent of iron at ~100 μM ΣH_2S. Water column sulfide concentrations sufficient for authigenic Mo-sulfide precipitation would therefore be limited to stations that lie below the chemocline, where oxygen is no longer detectable (Fig. 2; Edmond et al., 1993). Under current conditions, ΣH_2S in the water column reach a maximum of ~30 μM at depth, i.e. they remain below the APS (Fig. 2). However, dissolved S (H_2S and SO_4^{2-}) concentrations have likely varied in the past, and ΣH_2S concentrations could have been closer to the APS for Mo removal into sulfides.

Estimates of Mo enrichment in Tanganyika sediments show higher values below the chemocline (Fig. 4). Most of the Lake Tanganyika Mo data, with the exception of some deep pyrite-rich sediments, have an average Mo_{xs}:C_{org} ratio of ~3 μmol mol^{-1}. This ratio is lower (2.1 ± 0.5 μmol mol^{-1}, SDOM, $n = 31$) for the three shallowest sites above or within the chemocline but is higher for the deeper two sites along the Luiche Platform transect (3.4 ± 0.7 μmol mol^{-1}, SDOM, $n = 18$). The generally lower Mo_{xs}:C_{org} ratios observed in the sediments above or within the chemocline may reflect less efficient authigenic Mo capture or oxygen exposure at the shallower sites leading to inefficient Mo preservation. It is worth noting, however, that given the uncertainties in our lithogenic correction it is quite possible that our shallowest (oxygenated) site has only a small average Mo enrichment above the lithogenic background (Table 1).

In deeper sediments bathed in sulfidic waters, the uptake and preservation of Mo appears to increase (Fig. 4). The increase in Mo sediment concentration and the Mo_{xs}:C_{org} ratio with increasing water depth is roughly coincident with increases in water column dissolved sulfide content (cf. Figs. 2, 4 and 8), suggesting that sulfur chemistry may influence Mo burial even when water column ΣH_2S concentrations are below the APS. Despite a general correlation between authigenic Mo and C_{org} for sediments containing up to ~4 ppm Mo, sediments with higher Mo concentrations no longer fall along this trend (Fig. 8). We suspect that the high S_{inorg}, high Mo sediments reflect Mo precipitation associated with more intense S cycling during a past period of highly reducing lake chemistry (e.g., Fig. 4). However, because the enriched sedimentary Mo contents in many of the samples appear to coincide with high C_{org} concentrations, we suspect that the dominant pool of Mo present in these lake sediments is initially associated with organic material, particularly for the modern lake (Fig. 8, also see Algeo and Lyons, 2006). A clear distinction between primary (assimilatory) and secondary (syngenetic or diagenetic) Mo is not, strictly speaking, possible based on our data. However, it seems that there may well be an or-

ganic matter associated (assimilatory) Mo pool, which appears to have a Mo_{xs}/C_{org} of ~2–4 μmol Mo mol^{-1} C_{org}. This value is consistent with the shallower Luiche Platform sites, the deep core average during periods of low S_{inorg} (Appendix Table S2), and, more significantly, the approximate ratio seen for a number of organisms (e.g., Tuit et al., 2004; Glass et al., 2010). As the Mo_{xs} to C_{org} ratio increases, which occurs in the presence of high S_{inorg}, we postulate that Mo is being taken up in the sediments in association with pyrite or secondarily removed with organic matter. This particular logic follows the first Mo uptake point indicated for marine settings by Zheng et al. (2000).

Cadmium, like Mo, is also known to form associations with organic matter, and indeed Cd covaries with C_{org} along the Luiche Platform (Fig. 8). There is a biological association between Cd and C_{org} that has been shown for marine phytoplankton through a Cd-containing carbonic anhydrase (e.g., Price and Morel, 1990; Ho et al., 2003; Lane et al., 2005; Morel and Malcom, 2005; Park et al., 2007). Association of Cd with biological material is further suggested by the relatively invariant $Cd:C_{org}$ ratio reported for particulate marine organic matter ($Cd:C_{org}$ ratio of ~3 μmol mol^{-1}; Rosenthal et al., 1995; also see Morel and Malcom, 2005, who note an average cellular quota of 2 μmol Cd mol^{-1} C_{org}). Although most of the work demonstrating a biological requirement for Cd has been done on marine systems (Morel and Malcom, 2005), we assume that similar relationships exist in freshwater systems, and indeed Ji and Sherrell (2008) demonstrate Cd:C values consistent with the marine values for two freshwater phytoplankton species. In addition to its association with organic matter, Cd is also immobilized in the presence of trace levels of free sulfide (<5 μM), forming an insoluble CdS (McCorkle and Klinkhammer, 1991; Rosenthal et al., 1995; van Geen et al., 1995), and this process could also be contributing to Cd burial in Lake Tanganyika as suggested by their covariance (Fig. 8).

The potential association between Cd and sulfide implies that Cd, like Mo, may undergo a secondary uptake or preservation process within the sediments. As with many trace elements, Cd concentrations tend to be quite low in freshwater systems (e.g., Sterner et al., 2004; Morel and Malcom, 2005) and it is therefore not surprising that Lake Tanganyika sedimentary Cd enrichments are low when compared to the background levels for all sites in this study. The maximum estimated enrichment is only ~0.1 ppm in the deepest Luiche Platform sediments and ~0.3 ppm at the 900 m site (Appendix Table S2 and Fig. 8). Nevertheless, our estimates suggest some amount of Cd enrichment at all depths, increasing below the chemocline (Fig. 4). The Lake Tanganyika data all exhibit a $Cd:C_{org}$ burial ratio significantly below that typical of (marine) organic material, with the Platform sites having a $Cd_{xs}:C_{org}$ ratio of $\sim 70 \pm 60$ nmol mol^{-1} and the deeper site having an average ratio of $\sim 500 \pm 300$ nmol mol^{-1} (Table S2). The low $Cd_{xs}:C_{org}$ ratio in lake sediments may point to Cd limitation in the surface water, or they may indicate lower Cd requirements by the lake phytoplankton community with the potential for Cd substitution by other trace metals, such as Zn or Co (Gettins and Coleman, 1982; Price and Morel, 1990; Lee and Morel, 1995). In light of the observed $Cd_{xs}:C_{org}$ relationships, we suspect that organic matter-associated Cd likely play at least some role in the initial bulk Cd pool in Tanganyika sediments. However the higher $Cd_{xs}:C_{org}$ ratios at the deeper site may reflect increased Cd preservation associated with sulfur burial or a larger Cd reservoir during the past. Despite the higher Cd concentrations within the deeper sediments, we also note here that the Cd concentrations do not correlate with either organic carbon or sulfur (Fig. 8). Rather, these concentrations plateau at ~0.3 ppm further supporting the suggestion that water column Cd availability is limited relative to reactive organic carbon and sulfur.

In short, Cd behavior contrasts that of Mo in that Mo appears to undergo a secondary enrichment process in some of the deep lake sediments and tends to covary with organic carbon and sulfur throughout the system (Fig. 8). Cadmium, on the other hand, is enriched in the deep lake relative to the shallow lake, with a distinct offset between the shallower (modern) lake sediment and the deeper (older) lake sediment; however, despite these patterns the enrichments over the lithogenic value are nevertheless low. Therefore, although there might be some secondary enrichment of Cd, it is possible that all of the Cd that makes it to the sediments does so in association with organic matter (either as a bioassimilated component or as an adsorbed component) and that any Cd that is buried in an inorganic phase does so through a sink transfer process, e.g., from organic matter to the sulfide phase. Furthermore, the low $Cd_{xs}:C_{org}$ burial ratio might imply that the lake may be operating under a Cd deficiency.

Unlike Mo and Cd, U is not known to play a nutritional role for aquatic biota. However, U does exhibit systematic correlations with C_{org} in settling particles and sediments in the marine environment (e.g., Anderson et al., 1989, 1998; Zheng et al., 2002). The processes that govern this coupling are unclear, but some amount of U may be delivered to the sediments through sorption to organic matter in the water column (e.g., Anderson et al., 1989; Klinkhammer and Palmer, 1991; Zheng et al., 2002). Authigenic precipitation of U is achieved primarily through the reduction of soluble U(VI) to the more insoluble U(IV) at sediment Eh conditions similar to those required for Fe(III) reduction (e.g., Anderson et al., 1989; Klinkhammer and Palmer, 1991). This reduction is thought to be (at least in part) a biologically mediated process (e.g., Lovley et al., 1991; Wall and Krumholz, 2006), likely by Fe- or S-reducing microorganisms that can use U as an alternative energy source (Lovley et al., 1993).

Sediment U:Ti ratios generally increase with water depth (Fig. 4), and estimated authigenic U concentrations increase from an average of ~1 ppm at the shallowest site to a high value of ~5 ppm at the 900 m site (Appendix Table S2 and Fig. 4). The relationship between core average authigenic U and C_{org} yields a $U:C_{org}$ burial ratio of $\sim 2.0 \pm 0.2$ μmol mol^{-1} (SDOM, $n = 50$) for the Luiche Platform sites. At the 900 m site, we observe lower $U:C_{org}$ ratios in the deeper, C_{org}- and sulfur-rich interval as compared to the rest of the core (Appendix Table S2). We suspect that, as with Cd, this difference reflects a period in the past when there was either a significant draw-down of U

within the water column or the lake's dissolved U input was lower. As a point of reference, our measurements of dissolved U concentration in the overlying water of our shallow cores show that the modern lake U concentrations are indeed quite low, $\sim 1.1 \pm 0.2$ nM.

Unlike the other authigenic metals, Re does not have a recognized history of primary or secondary associations with C_{org} (Dolor et al., 2009) and its removal mechanism is not well understood. Previous work suggests that is does not react with particles in the water column (Nameroff et al., 2004), and, to our knowledge, Re is not known to be biologically active (Dolor et al., 2009). A previous investigation of Re in anoxic lake sediments from Eastern Canada argued that Re removal was achieved through reduction of aqueous $Re^{VII}O_4^-$ to $Re^{IV}(OH)_4$ in the presence of dissolved sulfide concentrations at μM levels to produce the precipitate $ReS_{2(s)}$ (Chappaz et al., 2008).

The observed Re:Ti ratios in Lake Tanganyika sediments suggest that significant Re enrichment is limited to the deepest lake sediments (Figs. 4 and 8). Along these lines, it is noteworthy that Re is the only metal that does not exhibit a consistent pattern of increasing enrichment with water depth in the Luiche Platform cores (Fig. 4). Furthermore, maximum estimated Re enrichments are <4 ppb for even the deepest Luiche Platform sediments, while the sediments from the 900 m core have Re enrichments as high as ~11 ppb (Appendix Table S2). Given the uncertainty associated with the estimated lithogenic Re:Ti ratio, and the general lack of data on Re in crustal materials, it remains a possibility that samples of the Luiche Platform have only a lithogenic Re contribution, with authigenic Re accumulation being limited to the 900 m site (Fig. 4). The positive relationship between Re and sulfur burial in deep Lake Tanganyika sediments (Fig. 8) suggests that authigenic Re enrichment may be achieved through ReS_2 precipitation. Similarities between the Cd and Re enrichments versus S_{inorg} (Fig. 8, bottom panels), most notably the observation that both metals appear to reach a plateau above which enrichments seem decoupled from S_{inorg}, suggests that Re too is limited in the lake and that the lake's reservoir of dissolved Re is sufficiently low that it precludes a relationship with either C_{org} or S_{inorg}.

3.2.5. The Tanganyika trace metal record from ~5 to 18 ky

Our 900 m core covers a time period from approximately the end of the last glacial period (18 ky) to ~5 ky BP. Prior work has emphasized that there are relatively large fluctuations in biogenic silica and C_{org} contents that occurred during part of this period (Fig. 9; Felton et al., 2007; Tierney and Russell, 2007). Tierney and Russell (2007) interpreted these fluctuations as changes in the lake's ecology, where high biogenic silica represents periods of diatom production while high organic carbon periods are dominated by nitrogen fixing organisms. These authors further inferred that shifts in the dominant lake biota reflect changes in local wind stress, such that high diatom periods reflect upwelling (high wind) conditions and C_{org}-rich periods represent non-upwelling (low wind) conditions.

Although the resolution of our sampling does not match that of Tierney and Russell (2007), we note a general correspondence between our C_{org} values and their data (Fig. 9). Our data demonstrate that the period prior to about 11 ky was characterized by generally higher sedimentary organic carbon and sulfur contents. At ~11 ky, both C_{org} and S_{inorg} decrease, coincident with a regional increase in rainfall (Bonnefille and Chaliè, 2000; Tierney et al., 2008). Both C_{org} and S_{inorg} then remain low until ~6 ky, when both records return to higher values (Fig. 9). One possible interpretation of the higher C_{org} periods (relative to biogenic silica) is that lake mixing was less efficient because of lower wind speeds (Tierney and Russell, 2007). If this interpretation is correct, then during these periods nitrogen fixing organisms may have played a more important role in lake ecology as compared to the low C_{org} period from ~11 to 6 ky (Fig. 9; Tierney and Russell, 2007).

If indeed there are periods of dominance by nitrogen-fixing organisms, it is worth recognizing that this process

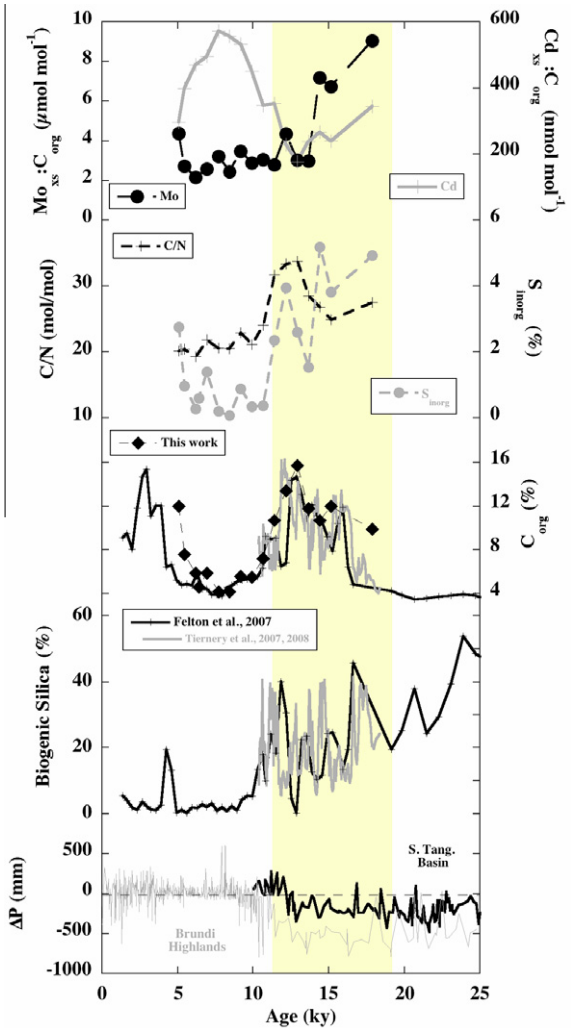

Fig. 9. Mo:C_{org}, Cd:C_{org}, C/N, C_{org}, S_{inorg}, ΔP (precipitation change), and % Biogenic Silica plotted as a function of time. Note that data points from 35.5 cm and deep turbidite layers are not included in this figure. Also note that C_{org} and biogenic silica data from Tierney and Russell (2007), Tierney et al. (2008), and Felton et al. (2007) are also plotted for comparison. ΔP (change in precipitation) data are taken from Bonnefille and Chaliè (2000).

requires higher Fe and Mo availability (e.g.,Tuit et al., 2004; Mendel and Bittner, 2006; Glass et al., 2009), which is consistent with the observed Mo enrichment relative to the modern Mo distributions for the period between ~14 and 18 ky (Fig. 9). It is possible that the original C_{org} from this period might actually be enriched in Mo because the original biological community had a higher demand due to enhanced nitrogen fixation. This period is followed by a decrease to more typical lake values, with a smaller secondary peak at ~12 ky (Fig. 9). The sedimentary Mo enrichments are coincident with S_{inorg} enrichments (Fig. 8) and it is tempting to speculate that these Mo enrichments relative to C_{org} ultimately reflect secondary sedimentary uptake of Mo into reduced sulfur phases.

For both U and Cd, the metal:C_{org} ratios are lower during the high sulfur periods of the lake (Fig. 9). In terms of biosynthesis, the low Cd:C_{org} ratios are particularly striking. If freshwater phytoplankton require substantial Cd similar to marine phytoplankton (Ji and Sherrell, 2008), Cd could have been a limiting trace element in the lake. The inference that Lake Tanganyika underwent a period of metal limitation is analogous to the previous predictions made for chemical evolution of the early Earth (Anbar and Knoll, 2002; Saito et al., 2003; Zerkle et al., 2005). In short, we speculate that trace metal enrichments during the reducing period (~18–11 ky) are muted because the lake's trace metal reservoirs are depleted during this period of high productivity. During the less reducing less productive period (~11–6 ky) on the other hand, trace metal concentrations are lower because sequestration mechanisms are ineffective.

It is also noteworthy that the C:N ratios change through the record, reaching particularly high values around 12 ky. Although the general sense from the literature is that most of the organic matter within the lake is autochthonous (Talbot et al., 2006; Felton et al., 2007) these high ratios may be signaling a period where terrestrial carbon input may be important. With this in mind, it is possible that some of the patterns in carbon and trace metal to C_{org} ratios are being impacted by variations in the contribution of terrestrial carbon.

4. CONCLUSIONS

Our sample sites cover a range of oxidation–reduction conditions from sediments overlain by lake waters containing oxygen, to lake waters having sulfide concentrations of ~30 μM. This range in electron transport potential allows us to infer the approximate sequence of trace metal burial in this lacustrine system. It appears that U enriches earliest in the sequence of electron transport, followed by Cd and then Mo. This initial sequence is supported by the enrichment of U at the shallowest site, but the correspondingly low enrichment in Mo and Cd for some samples. Given that Cd and Mo enrichments are low at this shallow site, it is possible that their enrichment (or preservation) is limited by the presence of water column oxygen. In effect, both the Cd and Mo to C_{org} ratios increase from the shallowest site to the subsequent site. The overall general covariation of Mo and Cd with C_{org} raises the possibility that their metal enrichments may arrive at the sediment–water boundary in association with organic matter, possibly as an assimilatory fraction. Re enrichment, by contrast, is quite small and ambiguous. All of the Re data seem to be in excess of a terrestrial background, however, that background is not well characterized. It is possible that Re is last in this sequence for significant enrichment, seeming to require lake sulfide concentrations of 30 μM or more. Like U, Re does not seem to participate in a biological function, but unlike U, Re is probably not delivered to the sediment in association with an organic carrier and is instead only taken up by the sediment in association with sulfide (e.g., Chappaz et al., 2008).

Lake Tanganyika has experienced at least two periods of highly reducing conditions since the last glacial. The first followed the last glacial period and ends at ~11 ky, and the second occurred more recently (<6 ky) during the Holocene. The modern sulfidic lake sediments, as represented by our 335 m site, imply that current conditions are less reducing than during the immediate post-glacial period. During the initial post-glacial interval, it appears that the dissolved reservoir for selected trace metals might have been significantly diminished either through enhanced sedimentary removal or a diminished riverine supply, and if this idea is correct, variations in the trace metal reservoir could have impacted the evolutionary ecology of the lake.

ACKNOWLEDGMENTS

We would like to express our sincere gratitude to Andy Cohen, Kiram Lezzar, Catherine O'Reilly, Ellinor Michel, and Hudson Nkotagu for their support throughout this project. Our project was made possible by their assistance, which was supported under the umbrella of an NSF-funded REU Nyanza Project. Without the infrastructure allowed by the NSF-supported project it would have been difficult to imagine completing this research. The assistance of Kiram Lezzar, in particular, throughout our field campaign was nothing short of heroic. Catherine O'Reilly supported collection of the CTD data through NSF Grant DBI 0608774. In addition multiple students associated with the REU Nyanza project were enthusiastic in lending a hand during our fieldwork, and we appreciate their contributions. We would also like to thank the captain and crew of the M/V Maman Benita for their assistance. Andy Ungerer, Rob Wheatcroft, Anna Pakenham, and Rhea Sanders all provided analytical support for this project. We would also like to thank Hans Brumsack, two anonymous reviewers and the AE, Tim Shaw for their constructive comments on this manuscript. The radiocarbon analyses were done at the NOSAMS analytical facility, which is supported by the National Science Foundation (NSF) under the Cooperative Agreement number, 0753487. Primary funding for this work was provided by NSF Grants 0518322 and 0551605 to J.M. and 0551716 to S.S. and T.W.L. Additional support was provided by NSF Grant 0721102 to J.M., which helped support RPB during the writing of this manuscript.

APPENDIX A. SUPPLEMENTARY DATA

Supplementary data associated with this article can be found, in the online version, at doi:10.1016/j.gca.2010.09.041.

REFERENCES

Algeo T. J. and Lyons T. W. (2006) Mo-TOC covariation in modern anoxic marine environments: implications for analysis of paleoredox and -hydrographic conditions. *Paleoceanography* **21**. doi:10.1029/2004PA001112.

Anbar A. D. and Knoll A. H. (2002) Proterozoic ocean chemistry and evolution: a bioinorganic bridge? *Science* **297**, 1137–1142.

Anderson R. F., Fleisher M. Q. and Lehuray A. P. (1989) Concentration, oxidation-state, and particulate flux of uranium in the Black-Sea. *Geochim. Cosmochim. Acta* **53**, 2215–2224.

Anderson R. F., Kumar N., Mortlock R. A., Froelich P. N., Kubik P., Dittrich-Hannen B. and Sutter M. (1998) Late-quaternary changes in productivity of the Southern Ocean. *J. Mar. Syst.* **17**, 497–514.

Anderson T. F. and Raiswell R. (2004) Sources and mechanisms for the enrichment of highly reactive iron in euxinic Black Sea sediments. *Am. J. Sci.* **304**, 203–233.

Barnett P. R. O., Watson J. and Connelly D. (1984) A multiple corer for taking virtually undisturbed samples from shelf, bathyal, and abyssal sediments. *Oceanol. Acta* **7**, 399–408.

Barrat J. A., Boulègue J., Tiercelin J. J. and Lesourd M. (2000) Strontium isotopes and rare-earth element geochemistry of hydrothermal carbonate deposits from Lake Tanganyika, East Africa. *Geochim. Cosmochim. Acta* **64**, 287–298.

Berner R. A. and Raiswell R. (1984) C/S method for distinguishing freshwater from marine sedimentary rocks. *Geology* **6**, 365–368.

Bonnefille R. and Chaliè F. (2000) Pollen-inferred precipitation time-series from equatorial mountains, Africa, the last 40 kyr BP. *Global Planet. Change* **26**, 25–50.

Brown E. T., Le Callonnec L. and German C. R. (2000) Geochemical cycling of redox-sensitive metals in sediments from Lake Malawi: a diagnostic paleotracer for episodic changes in mixing depth. *Geochim. Cosmochim. Acta* **64**, 3515–3523.

Brumsack H.-J. (2006) The trace metal content of recent organic carbon-rich sediments: implications for Cretaceous black shale formation. *Palaeogeogr. Palaeoclimatol. Palaeoecol.* **232**, 344–361.

Chappaz A., Gobeil C. and Tessier A. (2008) Sequestration mechanisms and anthropogenic inputs of rhenium in sediments from Eastern Canada lakes. *Geochim. Cosmochim. Acta* **72**, 6027–6036.

Cohen A. S., Dettman D. L., Talbot M. R., Awramik S. M. and Abell P. (1997) Lake level and paleoenvironmental history of Lake Tanganyika, Africa, as inferred from late Holocene and modern stromatolites. *GSA Bull.* **109**, 444–460.

Craig H. (1974) *Lake Tanganyika Geochemical and Hydrographic Study: 1973 Expedition*. Scripps Institution of Oceanography, UC San Diego. Available from: <http://www.escholarship.org/uc/item/4ct114wz San Diego>.

Degens E. T., Herzen R. P. and Wong H.-K. (1971) Lake Tanganyika: water chemistry, sediments, geological structure. *Naturwissenschaften* **58**, 229–241.

Dolor M. K., Gilmour C. C. and Helz G. R. (2009) Distinct microbial behavior of Re compared to Tc: evidence against microbial Re fixation in aquatic sediments. *Geomicrobiol. J.* **26**, 470–483.

Edmond J. M., Stallard R. F., Craig H., Craig V., Weiss R. F. and Coulter G. W. (1993) Nutrient chemistry of the water column of Lake Tanganyika. *Limnol. Oceanogr.* **38**, 725–738.

Erickson B. E. and Helz G. R. (2000) Molybdenum (VI) speciation in sulfidic waters: stability and lability of thiomolybdates. *Geochim. Cosmochim. Acta* **64**, 1149–1158.

Fairbanks R. G., Mortlock R. A., Chiu T.-C., Kaplan A., Guilderson T. P., Fairbanks T. W. and Bloom A. L. (2005) Marine radiocarbon calibration curve spanning 0 to 50,000 years B.P. based on paired $^{230}Th/^{234}U/^{238}U$ and ^{14}C dates on pristine corals. *Quat. Sci. Rev.* **24**, 1781–1796.

Felton A. A., Russell J. M., Cohen A. S., Baker M. E., Chesley J. T., Lezzar K. E., McGlue M. M., Pigati J. S., Quade J., Curt Stager J. and Tiercelin J. J. (2007) Paleolimnological evidence for the onset and termination of glacial aridity from Lake Tanganyika, Tropical East Africa. *Palaeogeogr. Palaeoclimatol. Palaeoecol.* **252**, 405–423.

Fossing H. and Jørgensen B. B. (1989) Measurement of bacterial sulfate reduction and sediments: evaluation of a single-step chromium reduction method. *Biogeochemistry* **8**, 223–245.

Froelich P. N., Klinkhammer G. P., Bender M. L., Luedtke N. A., Health G. R., Cullen D., Dauphin P., Hammond D. E., Hartman B. and Maynard V. (1979) Early organic matter in pelagic sediments of the eastern equatorial Atlantic: suboxic diagenesis. *Geochim. Cosmochim. Acta* **43**, 1075–1090.

Gettins P. and Coleman J. E. (1982) ^{113}Cd NMR of Cd(II)-substituted Zn(II) metalloenzymes. *Fed. Proc.* **41**, 13.

Glass J. B., Wolfe-Simon F. and Anbar A. D. (2009) Coevolution of metal availability and nitrogen assimilation in cyanobacteria and algae. *Geobiology* **7**, 100–123.

Glass J. B., Wolfe-Simon F., Elser J. J. and Anbar A. D. (2010) Molybdenum–nitrogen co-limitation in freshwater and coastal heterocystous cyanobacteria. *Limnol. Oceanogr.* **55**, 667–676.

Goldman C. R. (1960) Molybdenum as a factor limiting primary productivity in Castle Lake, California. *Science* **132**, 1016–1017.

Haberyan K. A. and Hecky R. E. (1987) The late Pleistocene and Holocene stratigraphy and paleolimnology of Lakes Kivu and Tanganyika. *Palaeogeogr. Palaeoclimatol. Palaeoecol.* **61**, 169–197.

Helz G. R., Miller C. V., Charnock J. M., Mosselmans J. F. W., Pattrick R. A. D., Garner C. D. and Vaughan D. J. (1996) Mechanism of molybdenum removal from the sea and its concentration in black shales: EXAFS evidence. *Geochim. Cosmochim. Acta* **60**, 3631–3642.

Ho T.-Y., Quigg A., Finkel Z. V., Milligan A. J., Wyman K., Falkowski P. G. and Morel F. M. M. (2003) The elemental composition of some marine phytoplankton. *J. Phycol.* **39**, 1145–1159.

Howarth R. W. and Cole J. J. (1985) Molybdenum availability, nitrogen limitation and phytoplankton growth in natural waters. *Science* **229**, 653–655.

Huc A. Y., LeFournier J., Vandenbroucke M. and Bessereau G. (1990) Northern Lake-Tanganyika – an example of organic sedimentation in an Anoxic Rift Lake. In *Lacustrine Basin Exploration, Case Studies and Modern Analogs* (ed. B. J. Katz). AAPG Memoir, pp. 169–185.

Hutchinson G. E. (1957) *A Treatise on Limnology*. Wiley, New York.

Ji Y. and Sherrell R. M. (2008) Differential effects of phosphorus limitation on cellular metals in Chlorella and Microcystis. *Limnol. Oceanogr.* **53**, 1790–1804.

Kimbadi S., Vandelannoote A., Deelstra H., Mbemba M. and Ollevier F. (1999) Chemical composition of the small rivers of the north-western part of Lake Tanganyika. *Hydrobiologia* **407**, 75–80.

Klinkhammer G. P. and Palmer M. R. (1991) Uranium in the oceans – where it goes and why. *Geochim. Cosmochim. Acta* **55**, 1799–1806.

Lane T. W., Saito M. A., George G. N., Pickering I. J., Prince R. C. and Morel F. M. M. (2005) Biochemistry: a cadmium enzyme from a marine diatom. *Nature* **435**, 42.

Lee J. G. and Morel F. M. M. (1995) Replacement of zinc by cadmium in marine phytoplankton. *Mar. Ecol. Prog. Ser.* **127**, 305–309.

Lovley D. R., Phillips E. J. P., Gorby Y. A. and Landa E. R. (1991) Microbial reduction of uranium. *Nature* **350**, 413–416.

Lovley D. R., Roden E. E., Phillips E. J. P. and Woodward J. C. (1993) Enzymatic iron and uranium reduction by sulfate-reducing bacteria. *Mar. Geol.* **113**, 41–53.

Lyons T. W. and Severmann S. (2006) A critical look at iron paleoredox proxies based on new insights from modern euxinic marine basins. *Geochim. Cosmochim. Acta* **70**, 5698–5722.

McCorkle D. C. and Klinkhammer G. P. (1991) Porewater cadmium geochemistry and the porewater cadmium:[delta]13C relationship. *Geochim. Cosmochim. Acta* **55**, 161–168.

Mendel R. R. and Bittner F. (2006) Cell biology of molybdenum. *Biochim. Biophys. Acta* **1763**, 621–635.

Morel F. M. M. (2008) The co-evolution of phytoplankton and trace element cycles in the oceans. *Geobiology* **6**, 318–324.

Morel F. M. M. and Malcom E. G. (2005) The biogeochemistry of cadmium. In *Metal Ions in Biological Systems: Biogeochemical Cycles of Elements* (eds. S. Astrid, H. Sigel and R. K. O. Sigel). Taylor & Francis Group, Boca Raton, FL, pp. 195–219.

Nameroff T., Calvert S. E. and Murray J. W. (2004) Glacial–interglacial variability in the eastern tropical North Pacific oxygen minimum zone recorded by redox-sensitive trace metals. *Paleoceanography* **19**, PA1010. doi:10.1029/2003PA000912.

Park H., Song B. and Morel F. M. M. (2007) Diversity of the cadmium-containing carbonic anhydrase in marine diatoms and natural waters. *Environ. Microbiol.* **9**, 403–413.

Poulson, R. (2008) The influence of early diagenesis on trace element and molybdenum isotope geochemistry. Ph. D. thesis, Oregon State University, 211pp.

Price N. M. and Morel F. M. M. (1990) Cadmium and cobalt substitution for zinc in a marine diatom. *Nature* **344**, 658–660.

Raiswell R., Buckley F., Berner R. A. and Anderson T. F. (1988) Degree of pyritisation of iron as a paleoenvironmental indicator of bottom-water oxygenation. *J. Sediment. Petrol.* **58**, 812–819.

Rosenthal Y., Lam P., Boyle E. A. and Thomson J. (1995) Authigenic cadmium enrichments in suboxic sediments: precipitation and postdepositional mobility. *Earth Planet. Sci. Lett.* **132**, 99–111.

Rudnick R. L. and Gao S. (2004) Composition of the continental crust. In *Treatise on Geochemsitry* (eds. H. D. Holland and K. K. Turekian). Elsevier, Amsterdam, pp. 1–64.

Saito M. A., Sigman D. M. and Morel F. M. M. (2003) The bioinorganic chemistry of the ancient ocean: the co-evolution of cyanobacterial metal requirements and biogeochemical cycles at the Archean/Proterozoic boundary? *Inorgan. Chim. Acta* **356**, 308–318.

Severmann S., Lyons T. W., Anbar A., McManus J. and Gordon G. (2008) Modern iron isotope perspective on Fe shuttling in the Archean and the redox evolution of ancient oceans. *Geology* **36**, 487–490.

Sterner R. W., Smutka T. M., McKay R. M. L., Xiaoming Q., Brown E. T. and Sherrell R. M. (2004) Phosphorus and trace metal limitation of algae and bacteria in Lake Superior. *Limnol. Oceanogr.* **49**, 495–507.

Stoffers P. and Hecky R. E. (1978) Late Pleistocene–Holocene evolution of the Kivu-Tanganyika basin. *Spec. Publ. Int. Ass. Sediment.* **2**.

Talbot M., Jensen N., Lærdal T. and Filippi M. (2006) Geochemical responses to a major transgression in Giant African Lakes. *J. Paleolimnol.* **35**, 467–489.

Taylor S. R. and McLennan S. M. (1985) *The Continental Crust: Its Composition and Evolution*. Blackwell, Oxford.

Tiercelin J.-J., Pflumio C., Castrec M., Boulégue J., Gente P., Rolet J., Coussement C., Stetter K. O., Huber R., Buku S. and Mifundu W. (1993) Hydrothermal vents in Lake Tanganyika, East African, Rift system. *Geology* **21**, 499–502.

Tiercelin J.-J., Thouin C., Kalala T. and Mondeguer A. (1989) The discovery of sublacustrine hydrothermal activity and associated massive sulfides and hydrocarbons in the north Tanganyika trough, East African Rift. *Geology* **17**, 1053–1056.

Tierney J. E. and Russell J. M. (2007) Abrupt climate change in southeast tropical Africa influenced by Indian monsoon variability and ITCZ migration. *Geophys. Res. Lett.* **34**, L15709. doi:10.1029/2007GL029508.

Tierney J. E., Russell J. M., Huang Y., Damste J. S. S., Hopmans E. C. and Cohen A. S. (2008) Northern hemisphere controls on Tropical Southeast African Climate during the past 60,000 years. *Science* **322**, 252–255.

Tribovillard N., Algeo T. J., Lyons T. and Riboulleau A. (2006) Trace metals as paleoredox and paleoproductivity proxies: an update. *Chem. Geol.* **232**, 12–32.

Tribovillard N., Riboulleau A., Lyons T. W. and Baudin F. (2004) Enhanced trapping of molybdenum by sulfurized organic matter of marine origin in Mesozoic limestones and shales. *Chem. Geol.* **213**, 385–401.

Tuit C., Waterbury J. and Ravizza G. (2004) Diel variation of molybdenum and iron in marine diazotrophic cyanobacteria. *Limnol. Oceanogr.* **49**, 978–990.

van Geen A., McCorkle D. C. and Klinkhammer G. P. (1995) Sensitivity of the phosphate–cadmium–carbon isotope relation in the ocean to cadmium removal by suboxic sediments. *Paleoceanography* **10**, 159–169.

Vandelannoote A., Deelstra H. and Ollevier F. (1999) The inflow of the Rusizi River to Lake Tanganyika. *Hydrobiologia* **407**, 65–73.

Voegelin A. R., N‰gler T. F., Samankassou E. and Villa I. M. (2009) Molybdenum isotopic composition of modern and carboniferous carbonates. *Chem. Geol.* **265**, 488–498.

Wall J. D. and Krumholz L. R. (2006) Uranium reduction. *Annu. Rev. Microbiol.* **60**, 149–166.

Wijsman J. W. M., Middleburg J. J. and Heip C. H. R. (2001) Reactive iron in Black Sea sediments: implications for iron cycling. *Mar. Geol.* **172**, 167–180.

Zerkle A. L., House C. H. and Brantley S. L. (2005) Biogeochemical signatures through time as inferred from whole microbial genomes. *Am. J. Sci.* **305**, 467–502.

Zheng Y., Anderson R. F., Van Geen A. and Fleisher M. Q. (2002) Preservation of particulate non-lithogenic uranium in marine sediments. *Geochim. Cosmochim. Acta* **66**, 3085–3092.

Zheng Y., Anderson R. F., Van Geen A. and Kuwabara J. (2000) Authigenic molybdenum formation in marine sediments: a link to pore water sulfide in the Santa Barbara Basin. *Geochim. Cosmochim. Acta* **64**, 4165–4178.

Associate editor: Timothy J. Shaw